

Analysis of SAR for body-mounted mobile phones

Min-Young Park⁽¹⁾, Chea-Ok Ko⁽²⁾, Jeong-Ki Pack⁽³⁾

Department of Radio Science and Engineering, Chungnam National University, Daejeon, KOREA.

mypark@cnu.ac.kr⁽¹⁾, wall081@cnu.ac.kr⁽²⁾, jkpack@cnu.ac.kr⁽³⁾

ABSTRACT

Due to the rapid growth of mobile communication users, many studies have been performed and currently ongoing on the biological effects of mobile-phone EMF. In this study, we have performed a dosimetric analysis for a mobile phone of head-mounted display type, which could also be a terminal of a wearable computer, and a wristwatch-type phone, to investigate possible biological effects of these devices. SAR (Specific Absorption Rate) distribution was calculated using FDTD (Finite Difference Time Domain) method, for adult human models, standard Korean human model and VHP(Visible Human Project) model, as well as scaled models. It has been found that these devices could cause some biological effects for children even with relatively low power.

Index Terms : body-mounted device, mobile phone, SAR, EMF, FDTD, dosimetry

INTRODUCTION

Recently mobile communication users have been growing very rapidly, and thus many studies have been performed and currently ongoing on the biological effects of mobile-phone EMF. There has been active development of new and advanced portable devices, and many efforts have also been directed to wearable computers with communication capability. Many such devices are commercially available now in market. So, it is necessary to investigate possible health effects of these devices on human body.

In this study, we have performed a dosimetric analysis for a mobile phone of head-mounted display type, which could also be served as a terminal of a wearable computer, and a wristwatch-type phone, to investigate possible biological effects of these devices. Typical commercial devices currently in market have been benchmarked.

To see the effects of these devices for different races and ages, SAR distributions for three different human models, VHP(Visible Human Project) adult model, child model(down-scaled VHP model) and Korean adult model, were calculated with SEMCAD and XFDTD, changing the position of antenna or device.

COMMERCIAL TREND OF BODY-MOUNTED MOBILE PHONES/TERMINALS

Recently, body-mounted or wearable mobile phones/terminals have been actively developed, and various systems are commercially available now in market. In commercial head-mounted display terminals, there are two types of systems for interconnection of main unit and terminal, wired and wireless. The Poma system of Xybernaut Co. is a wired type, and the MicroOptical's DV-1 system is a wireless type. The latter one was chosen for our analysis. Another type of commercial body-mounted device is wristwatch-type phones. The Samsung's GPRS wristwatch phone currently in market was modeled and simulated.

SIMULATION RESULTS FOR HEAD-MOUNTED DISPLAY

As a typical example of head-mounted display, the MicroOptical's DV-1 wireless digital viewer was modeled as shown in Fig. 1. This display has a head-mounted structure with a built-in dipole antenna of 2.4 GHz in the side frame of the display. The electrical properties of the material used for simulation are given in Table 1.

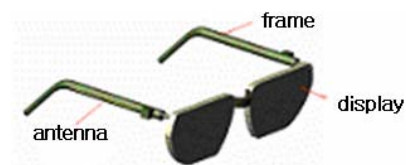


Fig. 1 The structure of head-mounted display.

Table.1 Electrical properties of the material used for modeling the head-mounted display.

| | Conductivity [S/m] | Dielectric constant |
|---------|-----------------------|------------------------|
| Display | 0.01 | 4.5 |
| Frame | 0.02 | 3.5 |

Fig. 2 shows the radiation pattern of the antenna built in the side frame of the display. Thin wire model was used for modeling, and the resulting antenna impedance is $85+j37.24$ ohms. The radiation efficiency, the ratio of radiated power and net input power, is 100 % and system efficiency, the ratio of available power and radiated power, is 86.82 %, respectively.

Since the SAR values inside a human body are normalized to the net input power in this paper, the values of impedance or antenna efficiency themselves are not important if the radiation pattern is same as that of real antenna.

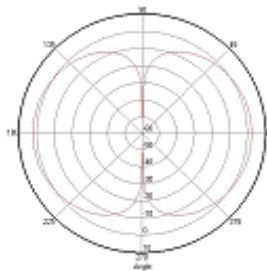


Fig. 2 Radiation pattern of the antenna in the head-mounted display.

Since eyeballs are more sensitive to heat compared to other parts of head, SAR distribution was calculated also when the antenna is located in the front frame of the display, to see the worst-case effects. In addition, to examine the differences in the absorbed power between races and ages, SAR distributions for VHP whole-body model, Korean whole-body model and down-scaled VHP model were simulated.

The voxel size of VHP whole-body model is 1 mm x 1 mm x 1 mm and the number of tissues is 110. To model the dielectric properties of the tissues, the FCC's tissue model was used. For 67 tissues among the 110 tissues, which are not defined in the FCC model, the dielectric properties of the most similar tissues were assigned. The voxel size of Korean whole-body model is 3 mm x 3 mm x 3 mm and the number of tissues is 29. The overall dimension of Korean adult model is smaller than that of

VHP adult model. For all models, including scaled model mentioned below, adaptive meshes were used in the region around antenna.

To model a child, a down-scaled VHP model was used. The size of VHP adult model and standard 13 year-old Korean boy (<http://sizekorea.ats.go.kr/>) are given in Table 2. Comparing the overall dimensions of the two, we chose the scale factor of 0.74 based on the size of head thickness. The height of the scaled model in this case is about 138 cm.

Table.2 Size of VHP adult model and standard 13 year-old Korean boy [mm].

| | VHP model | 13 year-old Korean model | Scale factor |
|-----------------|-----------|--------------------------|--------------|
| Chest thickness | 313.6 | 178.7 | 0.56 |
| Chest width | 549 | 260.9 | 0.48 |
| Height | 1870 | 1582.4 | 0.85 |
| Head thickness | 240 | 178.3 | 0.74 |
| Head width | 165 | 154.7 | 0.94 |
| Head length | 250 | 227 | 0.91 |

Fig. 3 shows the SAR distribution in the VHP adult model wearing the head-mounted display for the case of the antenna built in the side frame. SEMCAD was used for simulation. The maximum 1 g averaged SAR value is 13.15 W/kg/W in this case.

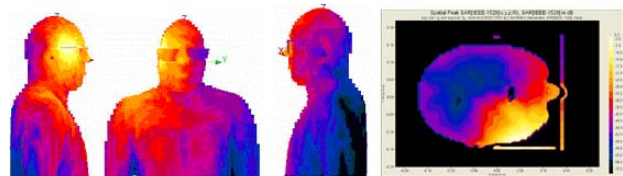


Fig. 3 SAR distribution in the VHP adult model when the antenna is located in the side frame.

Fig. 4 shows the SAR distribution in the VHP adult model when the antenna is located in the front frame. The maximum 1 g averaged SAR value is 23.82 W/kg/W, which is much larger than the previous case.

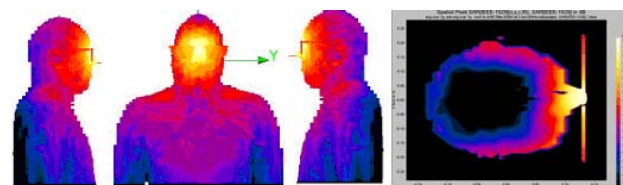


Fig. 4 SAR distribution in the VHP adult model when the antenna is located in the front frame.

The SAR distribution in the child model is given in Fig. 5. The maximum 1 g averaged SAR value is 17.44 W/kg/W, and it is also larger than that for the adult model.



Fig. 5 SAR distribution in the down-scaled VHP model when the antenna is located in the side frame.

The SAR distribution in Korean adult model calculated using XFDTD is shown in Fig. 6. The maximum 1 g averaged SAR is 15 W/kg/W. This larger value of SAR reveals the effects of size difference between the two adult models.

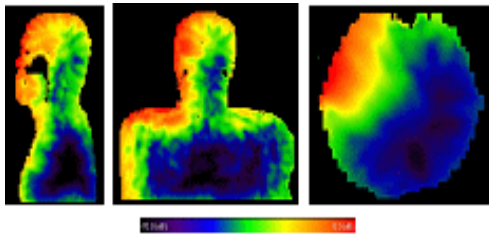


Fig. 6 SAR distribution in the Korean adult model when the antenna is located in the side frame.

SIMULATION RESULTS FOR WRISTWATCH-TYPE PHONE

As a typical commercial product of wristwatch-type phone, the Samsung's GPRS wristwatch phone was modeled, and the result is shown in Fig. 7. The antenna has the same curvature of the strap for wrapping around wrist and the operating frequency is 2.4 GHz. The electrical properties of each part used for simulation are given in Table 3.

The radiation pattern of the modeled antenna in the wristwatch phone is given in Fig. 8, and the antenna impedance is $92.94 + j48.84$ ohms. The radiation efficiency is 99.64 %, and the system efficiency is 81.31 %.

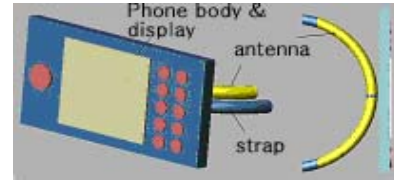


Fig. 7 Wristwatch type phone.

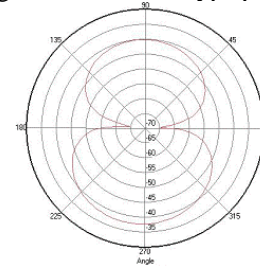


Fig. 8 Radiation pattern of the antenna in the wristwatch phone.

Table.3 Electrical properties of material used for modeling the wristwatch phone.

| | Conductivity [S/m] | Dielectric constant |
|------------|-----------------------|------------------------|
| Phone body | 0.04 | 4.0 |
| Strap | 0.0007 | 2.25 |
| Display | 0.01 | 4.5 |

Considering the positions of normal use and the worst-case position, simulations were performed locating the phone in mouth, heart, waist and thigh. As for the head-mounted display, SAR distributions were calculated for three different human models, the VHP adult model, the Korean adult model and the down-scaled VHP model.

The SAR distribution in the VHP adult model for the worst-case position in which the wristwatch phone is located in front of the mouth with the main beam oriented toward the face is shown in Fig. 9. The maximum 1 g averaged SAR is 5.23 W/kg/W, which is pretty much smaller than the SAR values for the head-mounted display.

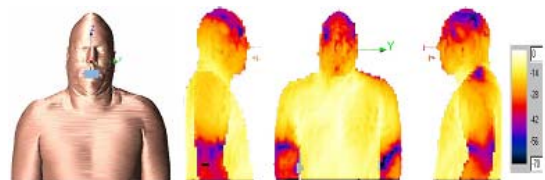


Fig. 9 SAR distribution in the VHP adult model when the wristwatch-type phone is located in front of the mouth.

The SAR distribution in the down-scaled VHP model

when the wristwatch phone is located in the waist is shown in Fig. 10. The maximum 1 g averaged SAR is 5.01 W/kg/W. All the other results are summarized in Table 4.

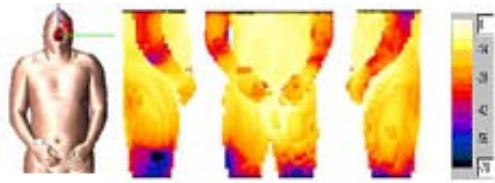


Fig. 10 SAR distribution in the down-scaled VHP model when the wristwatch-type phone is located in waist.

SUMMARY OF THE SIMULATION RESULTS

The maximum 1 g averaged SAR values for various cases, normalized to net input power, are summarized in Table 4.

Table.4 Summary of the maximum 1 g averaged SAR values [W/kg/W].

| Classification | Head-mounted display | | Wristwatch-type phone | | | |
|---------------------------------|----------------------|-------|-----------------------|-------|-------|-------|
| | Side | Front | Mouth | Heart | Waist | Thigh |
| VHP Adult | 13.15 | 23.82 | 5.23 | 2.33 | 6.38 | 2.49 |
| Child (VHP down-scaled by 0.74) | 17.44 | 35.79 | 6.24 | 6.29 | 5.01 | 6.38 |
| Korean Adult | 15.00 | 31.60 | 7.97 | 4.24 | 5.03 | 4.18 |

The results indicate that the maximum SAR values are higher for all cases in order of the smallness of the body size, that is child model, Korean adult model and VHP adult model, except for only one case in which the wristwatch phone is located in waist. This can be explained from the following observations. When the body size is small, the total absorbed power is small because it is proportional to the cross-sectional area of the exposed part of the body. The absorbed field, however, could be more localized which would lead to a higher local SAR, because the relative size of tissues for a small body is also reduced. In case of waist, on the other hand, the local SAR in the waist of a small body could be small, since there are no small organs and thus there is no significant localization.

CONCLUSIONS

In this paper, we analyzed the effects of commercially available head-mounted display and wristwatch-type phone on SAR distribution in three different human body models. Results indicate that 1 g averaged SAR values for head-mounted display could exceed 1.6 W/kg(the exposure limit of Korean regulation) when input power is 100 mW. If the input power is 10 mW, the normal power level of this type of devices, the SAR values for all cases are below 22 % of the exposure limit.

However, considering the fact that the body-mounted devices are turned on most of the time, and also the fact that eyes or reproductive organs, which are more likely to be the main exposure part, are relatively weak to EMF exposure, it seems that accurate dosimetric analysis and efforts for reducing exposure are required in the designing and developing stages of such devices.

ACKNOWLEDGEMENTS

This research was supported by the EMERC(ElectroMagnetic Environment Research Center) in Chungnam National University, one of IT Research Centers.

REFERENCES

- [1] A.K. Lee, H.D. Choi, K.Y. Cho, W.Y. Choi, and M.S. Chung, "Effects of the outer shape of a head on SAR evaluation of a mobile phone," BEMS 22th Annual Meeting Abstract Book, pp 130-131, June 11-16, 2000
- [2] A.K. Lee, H.D. Choi, H.S. Lee, and J.K. Pack, "Human head size and SAR characteristics for handset exposure," ETRI Jour. vol. 24, no. 2, pp 176-179, Apr. 2002.
- [3] "Eyeglass interface system", United States Patent 6,091,546, 2000.
- [4] Rekimoto J, "GestureWrist and GesturePad : Unobtrusive Wearable Interaction Devices", the Fifth International Symposium on Wearable Computers, 2001.